Flexible and Efficient Long-Range Planning Through Curious Exploration

Aidan Curtis [1] Minjian Xin [2] Dilip Arumugam [3] Kevin Feigelis [3] Daniel Yamins [3]

Abstract

Identifying algorithms that flexibly and efficiently discover temporally-extended multi-phase plans is an essential step for the advancement of robotics and model-based reinforcement learning. The core problem of long-range planning is finding an efficient way to search through the tree of possible action sequences. Existing non-learned planning solutions from the Task and Motion Planning (TAMP) literature rely on the existence of logical descriptions for the effects and preconditions for actions. This constraint allows TAMP methods to efficiently reduce the tree search problem but limits their ability to generalize to unseen and complex physical environments. In contrast, deep reinforcement learning (DRL) methods use flexible neural-network-based function approximators to discover policies that generalize naturally to unseen circumstances. However, DRL methods struggle to handle the very sparse reward landscapes inherent to long-range multi-step planning situations. Here, we propose the Curious Sample Planner (CSP), which fuses elements of TAMP and DRL by combining a curiosity-guided sampling strategy with imitation learning to accelerate planning. We show that CSP can efficiently discover interesting and complex temporally-extended plans for solving a wide range of physically realistic 3D tasks. In contrast, standard planning and learning methods often fail to solve these tasks at all or do so only with a huge and highly variable number of training samples. We explore the use of a variety of curiosity metrics with CSP and analyze the types of solutions that CSP discovers. Finally, we show that CSP supports task transfer so that the exploration policies learned during experience with one task can help improve efficiency on related tasks.

[1]Rice University [2]Shanghai Jiao Tong University [3]Stanford University. Correspondence to: Aidan Curtis <arc11@rice.edu>.

Proceedings of the 37^{th} International Conference on Machine Learning, Vienna, Austria, PMLR 108, 2020. Copyright 2020 by the author(s).

1. Introduction

Many complex behaviors such as cleaning a kitchen, organizing a drawer, or cooking a meal require plans that are a combination of low-level geometric manipulation and high-level action sequencing. Boiling water requires sequencing high-level actions such as fetching a pot, pouring water into the pot, and turning on the stove. In turn, each of these high-level steps consists of many low-level task-specific geometric action primitives. For instance, grabbing a pot requires intricate motor manipulation and physical considerations such as friction, force, etc. The process of combining low-level geometric decisions and high-level action sequences is often referred to as multi-step planning.

While high-level task planning and low-level geometric planning are difficult problems on their own, integrating them presents unique challenges that add further complexity. Task and Motion Planning (TAMP) is a powerful approach to the problem which constructs plans in logical terms that execute a sequence of macro-actions that are composed of geometric motion plans (Fikes & Nilsson, 1971; Dantam et al., 2016). While TAMP has been successful at generating temporally-extended multi-step plans that conform to geometric constraints, it requires actions to have defined preconditions and effects that modify the logical description of the world state. This is an unreasonable assumption for complex physical tasks because real-world effects and preconditions are often unknown or difficult to describe with logical predicates. These assumptions limit the flexibility and robustness of the TAMP approach. In addition, TAMP is computationally costly because it requires geometric motion planning for each macro-action sample.

In contrast, deep reinforcement learning (DRL) (Arulkumaran et al., 2017) methods have shown success at learning flexible policies for a variety of complex tasks in unstructured domains (Mnih et al., 2015; Lillicrap et al., 2015; Silver et al., 2016; Hessel et al., 2017; Vinyals et al., 2019). Central to the problem of reinforcement learning is the issue of exploration (Thrun, 1992; Kakade, 2003), whereby how an agent chooses to navigate its environment and acquire feedback signals has strong implications on the sample-efficiency of learning. Indeed, recent work in DRL has been plagued by large sample complexity stemming, in large part, from the challenge of exploration in sparse reward environments (Osband et al., 2016; Pathak et al., 2017; Riedmiller et al., 2018; Choi et al., 2019). Thus, sparse-reward tasks coupled with long-horizon planning becomes prohibitively difficult as highly-specific actions sequences must be executed prior to observing any nontrivial feedback. As such, developing flexible multi-step planning algorithms that operate under such constraints is an open challenge.

In this paper, we combine aspects of TAMP and DRL to achieve progress toward efficient and flexible long-horizon planning. We introduce the Curious Sample Planner (CSP), which uses curiosity (Schmidhuber, 2010; Pathak et al., 2017) to bias the search toward novel points in the state space. Our method combines the flexibility and transferability of DRL with the temporally-extended, multi-step planning of TAMP. We illustrate the power of CSP in a variety of qualitatively distinct problems in multi-step planning for which logical descriptions of action effects would be difficult to construct, including the building of complex structures and the discovery of simple machines for achieving challenging physical goals. We show CSP dramatically improves sample complexity compared to standard planning algorithms and DRL baselines which are, in most cases, unable to find a solution at all. We compare a variety of distinct curiosity metrics for use with CSP and demonstrate that dynamics-based curiosity performs well on tasks which require many dynamic object interactions while state-based curiosity performs better for structure-building tasks. Finally, we show that CSP can transfer between related but qualitatively distinct tasks, utilizing knowledge from one task to speed the solution of another.

2. Related Work

A classical approach to planning is that of sample-based geometric motion planners. Rapidly Exploring Random Trees (RRT) and Probabilistic Road Maps (PRM) combine goal-directed sampling with off-target sampling to balance exploration of the state space with exploitation of knowledge about the goal configuration (Lavalle, 1998; Kavraki et al., 1996). While these algorithms can work even for high dimensional configuration spaces, they are computationally intractable for tasks with the complex constraints that often exist in real world settings (Kingston et al., 2018). For a robotic manipulator, grasping an object has a necessary condition that the agent's manipulator is in a position to grasp that object. These constraint barriers in the configuration space render the goal-directed component of motion planning ineffective and necessitate a random exploration the entire configuration space. So while sample-based geometric motion planners are effective at simple tasks, they fail for temporally extended multi-step tasks with intricate constraints. We use sample-based geometric motion planners as a part of our solution to the multi-step planning problem.

More recently, Task and Motion Planning has shown success in developing temporally extended multi-step plans under both fully known and partially observed environment dynamics. A number of TAMP algorithms (Kaelbling & Lozano-Pérez, 2013; Gravot et al., 2005; Hertle et al., 2012; Srivastava et al., 2014) have solved tasks such as block stacking, object packing, table setting, and much more. TAMP algorithms generally iterate between a motion planning step using (e.g.) RRT or PRM, and a symbolic planning step using algorithms such as Fast Downward Planning (Helmert, 2006) or Fast Forward Planning (Hoffmann & Nebel, 2001).

However, a major roadblock for TAMP is that for each separate robot and environment, logical predicates describing the effects and preconditions of macro-actions must be manually derived. This limits the flexibility of any one TAMP implementation, since the predicates describing one setup are incompatible with those from another. In fact, direct performance comparison between existing TAMP algorithms is itself difficult for this reason, as highly variable environment and action specifications render any two TAMP solutions unrunnable in each other's domain without substantial work. This inflexibility is the *raison d'etre* of our work, but is also the reason we also cannot directly compare our solution to any specific TAMP implementation. Here, we take inspiration from TAMP by using geometric motion planners as subprocedures, but dramatically increase flexibility by using learning to intelligently sample generic macro-actions, avoiding the need for situation-specific predefined logical descriptions.

Other methods have been proposed to increase the efficiency and flexibility of Task and Motion Planning. Supervised learning of the preconditions and effects of certain macro-actions removes the need for manual specification, but requires constructing task-specific training datasets (Kroemer & Sukhatme, 2016; Wang et al., 2018). Other work has focused on factoring the planning problem into submanifolds with analytic constraints in order to reduce the size of the search space. (Garrett et al., 2018; Vega-Brown & Roy, 2018). TAMP can be accelerated by generating a sampling distribution around the goal trajectory using GANs (Kim et al., 2018) or by using reinforcement learning to learn search heuristics through expert examples or previously solved problem instances (Chitnis et al., 2016; Kim et al., 2019). In this work, we also introduce an algorithm that can utilize information gained from previous problem instances to speed up planning and generalize to related tasks. Instead of supervising on expert examples or task-specific training sets, we use self-supervision signal, allowing the agent to discover novel multi-step plans *de novo*.

Because multi-step long-range planning is a sparse reward environment, our use of reinforcement learning relies on the idea of intrinsic motivation (Singh et al., 2005; Kulkarni et al., 2016; Bellemare et al., 2016) to augment the environment reward signal with additional feedback. Empirically, intrinsic motivation has been shown to dramatically accelerate agent learning in such sparse-reward tasks (Burda et al., 2019). More recent work (Pathak et al., 2017; Achiam & Sastry, 2017; Haber et al., 2018) has gone on to leverage curiosity-based intrinsic motivation (from now on referred to as curiosity) to provide additional learning feedback in a self-supervised manner, without relying on hand-tuned auxiliary rewards. Our CSP approach utilizes DRL augmented by this same kind of curiosity signal in order to accelerate the classic tree-search-style planning methods commonly found in the TAMP literature, without inheriting the prequisite of specifying action preconditions and effects. Through our experiments, we study three distinct measures of curiosity (forward dynamics (Pathak et al., 2017), random network distillation (Choi et al., 2019), & state estimation (Mitash et al., 2017)) and examine their efficacy in synthesizing plans for a number of simulated robotics tasks with varying levels of difficulty.

Finally, much work has been done on building artificial robotic or simulated agents capable of exploring their environment, using tools, and solving physically realistic tasks (Toussaint et al., 2019; Nair et al., 2018; Deisenroth et al., 2011; Li et al., 2019). However, the algorithmic solutions used solve these tasks either involve manual specification of action effects and preconditions, tailored reward structures using curriculum learning, or expert demonstrations. To our knowledge, our work is the first example where such usages emerge from a flexible, generically applicable algorithm.

3. Mathematical Description

3.1. Problem Description

We begin by introducing the classic Markov Decision Process (MDP) formalism (Bellman, 1957; Puterman, 1994) denoted by $\mathcal{M} = \langle \mathcal{S}, \mathcal{A}, \mathcal{R}, \mathcal{T}, \gamma \rangle$, where $\mathcal{S}$ is a (potentially infinite) set of states, $\mathcal{A}$ is a (potentially infinite) set of actions, $\mathcal{R} : \mathcal{S} \times \mathcal{A} \to \mathbb{R}$ is a reward function, $\mathcal{T} : \mathcal{S} \times \mathcal{A} \to \mathcal{S}$ is a deterministic transition function, and $\gamma \in [0, 1)$ is a discount factor.

For the purposes of this work, we will augment the above MDP definition in two ways. First, the action space is replaced by a set of macro-actions $\mathcal{M}$ which, when selected, will be converted into an appropriate sequence of low-level actions in $\mathcal{A}$ using geometric motion planning and inverse kinematics. Second, we will assume that all tasks have an associated goal space $\mathcal{G} \subset \mathcal{S}$ where each $g \in \mathcal{G}$ can be viewed as a satisfactory terminal state, obviating the need for a reward function $\mathcal{R}$. Thus, we can concretely express an agent's goal as synthesizing a plan from some initial start state s_0 to navigate to any goal state in $\mathcal{G}$.

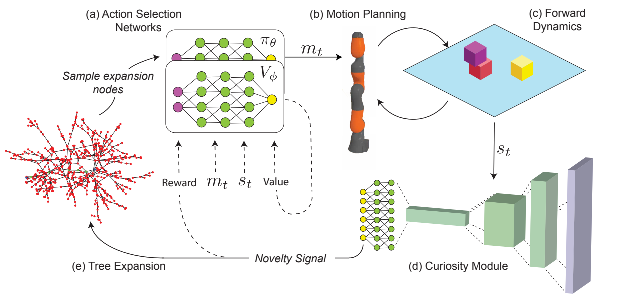

Figure 1. **a.** The action selection networks select actions that maximize curiosity. **b.** Parameterized macro-actions are converted to motion primitives. **c.** The forward dynamics module predicts the effects of executing those motor primitives in a particular state. **d.** The curiosity module represents the current world state and outputs one of the curiosity metrics (see section 4.4). **e.** The search tree is expanded.

3.2. Curious Sample Planner

Below, we describe the Curious Sample Planner. We first describe the CSP's system architecture, including its constituent neural networks and geometric planning module. We then describe the curious tree-search algorithm by which CSP uses these modules to construct multi-step plans.

System Architecture: CSP is comprised of four main modules (Fig. 1). The action selection networks include an actor-network $\pi_\theta : \mathcal{S} \to \mathcal{M}$ and a critic-network $V_\phi : \mathcal{S} \to \mathbb{R}$ (Fig. 1a), which learn to select macro-actions and choose parameters of that macro-action given a particular state. The action selection networks have two primary functions: maximizing curiosity in action selection and avoiding infeasible macro-actions. The networks are trained using actor-critic reinforcement learning (namely, Proximal Policy Optimization (PPO) (Schulman et al., 2017)) where π_θ has learnable parameters θ and V_ϕ has learnable parameters ϕ. The networks select feasible actions which maximize the novelty signal, leading to actions which result in novel configurations or dynamics. The actor network outputs a continuous (real-valued) vector which is translated into a macro-action with both discrete and continuous parameters. The forward dynamics module $f : \mathcal{S} \times \mathcal{A} \to \mathcal{S}$ (Fig. 1c) takes a state and an action primitive, simulates forward a fixed time τ, and returns the resulting state. This forward dynamics module is used by a geometric planning module (Fig. 1b) to convert macro-actions in $\mathcal{M}$ into feasible sequences of motor primitives in $\mathcal{A}$. Finally, the curiosity module is a neural network H_β (H stands for heuristic, Fig. 1d) that takes states as inputs and returns a curiosity score, with learnable parameters β. The exact input and output of the curiosity module is dependent on the type of curiosity being used (see §4.4).

CSP Algorithm: At its core, CSP is an algorithm for

Algorithm 1 The CSP algorithm.

```
Input: Initial state $s_0$, Goal set $\mathcal{G}$, dynamics $f$
Output: Path$\{(s_0, a_0, s_1), ..., (s_{n-1}, a_{n-1}, s_n)\}$ where
        $s_n \in G, f(s_i, a_i) = s_{i+1}$
1  $\mathcal{T} = (\{s_0\}, \emptyset)$
2  Randomly Initialize $\pi_\theta, V_\phi, H_\beta$
3  Initialize P$(s_0) = 1$
4  while $\mathcal{V} \cap G = \emptyset$ do
5      $S \leftarrow$ batch sample $\sim$ P$(\mathcal{V})$
6      $M \leftarrow \pi_\theta(S)$
7      $A =$ motion planning using $f$ for each $m \in M$
8      $S' \leftarrow f(S, A)$
9      $\mathcal{L} \leftarrow$ novelty metric
10     $\mathcal{L}(A = \emptyset) = 0$
11     Train $H_\beta$ to minimize $\mathcal{L}(\mathcal{A} \neq \emptyset)$
12     Update $\pi_\theta, V_\phi$ to maximize $\mathcal{L}$
13     $\mathcal{V} \leftarrow S' \cup \mathcal{V}$
14     Add each $(S_i, S'_i)$ to $\mathcal{E}$
15     P = softmax(novelty metric for each $v \in \mathcal{V}$)
   end
16 return Path in $\mathcal{T}$ from $s_0$to $s_g \in \mathcal{V} \cap G$
```

efficiently building a search tree over the state space using parameterized macro-actions (see Algorithm 1). The algorithm starts by initializing a tree $\mathcal{T} = (\mathcal{V}, \mathcal{E})$ in which the vertices are points in the continuous state space, edges are macro-actions with defined parameters, and paths are sequences of macro-actions which are guaranteed to transition between states at each end of the path under the dynamics model. The tree starts with a single vertex s_0 which is the start state of the multi-step planning problem. The algorithm also initializes a probability distribution over the tree vertices such that $P(s_0) = 1$. A batch of size B states are then sampled from P and passed into π_θ resulting in a set of state/macro-action pairings.

The next step of the algorithm is to convert the selected macro-actions into primitive action sequences using a combination of inverse kinematics and geometric motion planning. We use RRT-Connect (Kuffner & LaValle, 2000) for motion planning and the recursive Newton Euler algorithm (Luh et al., 1980) for inverse kinematics. The exact routine for converting macro-actions to primitives is specific to the macro-action. In some cases it is infeasible to convert macro-actions to motor primitives. (For example, it is infeasible to pick up an object that is out of the robot's reach.) In such cases, the planning module returns an empty sequence of primitives. These feasibility conditions are not explicitly represented as logical preconditions, but are discovered from failed attempts at inverse kinematics or motion planning. Over time, the action selection network learns to focus only on feasible macro-actions. The resulting sequence of action primitives are passed into the black-box dynamics module to get a corresponding batch of future states.

In order to determine which states and actions should be further explored, the algorithm creates a curiosity score for each of the selected macro-actions. Passing the batch of states and future states through the curiosity module will give a prediction loss, or novelty score. A subset of the new states with high novelty scores in the batch are then added as vertices in the search tree and the probability distribution P is adjusted to give more weight to states with high novelty scores. Although it is not strictly necessary for CSP to function, for increased computational efficiency we discard vertices with low probability (typically the bottom 90% of the distribution), as they are extremely unlikely to be sampled. After scores are calculated, the input states that have infeasible macro-actions are given a curiosity score of zero, strongly disincentivizing infeasible macro-action selection. The curiosity module is trained from the losses generated by the batch and the novelty score is used as the reward for the training of the action selection networks. This process repeats until the algorithm reaches a state in the goal subset or is exogenously terminated.

4. Experiments

4.1. Setup

Our experiments focus on a mounted robot arm with seven bounded revolute joints resulting in a seven dimensional configuration space, with fully-extended length r. The larger state-space $\mathcal{S}$ also includes (in addition to the robot joint angles) the total description of the positions and orientations of the dynamic and static objects, as well as their velocities, masses, and shapes, together with any (possibly dynamic) state-space constraints such as links or joints that may (permanently or temporarily) exist between objects in the environment.

Our robot's action primitives $\mathcal{A}$ consist of (1) a 7-dimensional continuous rotation space composed by linearly interpolating between θ_1 and θ_2 where θ_1, θ_2 are 7-vectors corresponding to bounds on each rotational degree of freedom, and (2) the ability to add a link constraint between any two objects in the environment, as long as the objects are touching and the robot arm is sufficiently close to both. We use Bullet (Coumans, 2015), a flexible physics simulation library, to execute robot actions in simulation. The environment and motion planning primitives were adapted from the pybullet-planning library (Garrett, 2018). The robot has access to a `PickPlace` macro-action which takes a target object, a goal position, and a goal orientation as input, and moves the target block to the goal position and orientation. The robot also has access to `AddConstraint` macro which takes two target objects as input, moves them into position for linking, and performs the link; and a corresponding `RemoveConstraint` that breaks the link if the objects are connected. While this setup is fairly typical of robotics applications, recall that our CSP algorithm makes no assumptions about the effects of actions on objects in the environment, and so our method could be applied to more complicated environments containing soft-body objects, cloths, and multiple robotic manipulators.

The robot must use its actions and macro-actions to achieve a goal, for example, moving a dynamic object D_i outside the reachable radius r of the robot would be defined by $G = \{s \in \mathcal{S} | {D_{i_x}}^2 + {D_{i_y}}^2 > r^2\}$. Though this type of goal definition is very simple and natural, finding a solution to such a task require complex strategic planning — *e.g.* perhaps requiring the discovery and construction of a simple machine, such as a ramp that could be used to slide the block out of the robot's reach (see section 4.2).

Finally, in this work, we assume an oracle dynamics model $f(s, a) = \mathcal{T}(s, a)$ and provide the robot with direct access to the underlying Bullet physics simulator. We leave the task of removing this assumption and employing a learned, approximate dynamics model (for instance, that model proposed in Mrowca et al. (2018)) to future work.

4.2. Tasks

Each of the four task types below are extremely easy to specify in the non-restrictive goal semantics accepted by CSP, but often require complex multi-step planning to solve, and would be extremely statistically improbable to be solved through random exploration. From a DRL point of view, such tasks correspond to extremely sparse reward landscapes. They also involve complex and fairly precise continuous motor manipulation of both rigid and non-rigid objects, using sequences of macro-actions whose preconditions would be very challenging to specify using logical predicates. The task set also affords some natural opportunities for cross-task transfer (e.g. between tower-building in **Block-Stack** and ramp building for **Push-Away**).

Block-Stack: In this task, the robot is provided with a set of K cubic blocks of size h, and the robot's goal is to cause at least one block to stably remain in position at z-position of greater than $(K - 1) * h$, without being in contact with the robot arm, for at least two seconds. Of course, the only feasible way for the robot to solve this problem is to stack the K blocks in a stable tower, but the robot is not provided with any reward at intermediate unsolved conditions. Block stacking is a commonly used task for evaluating planning algorithms because it requires detailed motor control and has a goal that is sparse in the state space.

Push-Away: In this task, the robot is provided with several large cubic blocks, a flat elongated block, and one additional

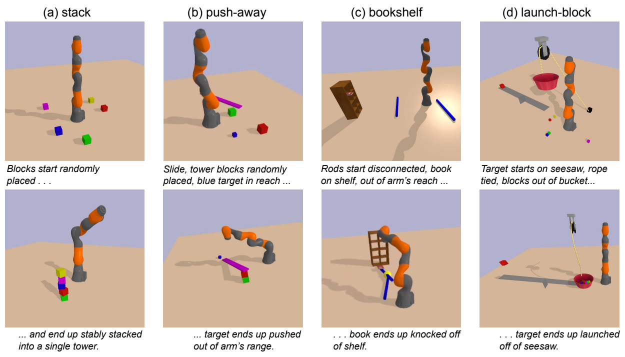
(a) stack
(b) push-away
(c) bookshelf
(d) launch-block
Blocks start randomly placed . . .
Slide, tower blocks randomly placed, blue target in reach ...
Rods start disconnected, book on shelf, out of arm's reach ...
Target starts on seesaw, rope tied, blocks out of bucket...
... and end up stably stacked into a single tower.
... target ends up pushed out of arm's range.
. . . book ends up knocked off of shelf.
. . . target ends up launched off of seesaw.

Figure 2. Visualizations each of the four task categories used to test CSP. Top Row: representative initial state for each task. Bottom Row: representative final state for each task. The **Block-Stack** task requires the robot to find a way to cause one block to remain stably at a high z-position without touching the arm, necessitating the building of a tower. The **Push-Away** task requires the robot to push the small (blue) block beyond the reach of the robot arm, which, depending on the circumstance might require the robot to build a ramp. The **Bookshelf** tasks requires the robot to knock a book off a shelf which is further away from the robot that it can reach, necessitating that the robot discover how to build a simple tool from the provided blue rods. The **Launch-Block** task requires the robot to launch the small red block off the far end of the seesaw, but it can only do so by putting all five of the other blocks as counterweight into the red bucket and detaching the pulley rope. Tasks are described in more detail in Section 4.2.

smaller "target" object that can be of variable shape (e.g. a cube or a sphere) and material (with e.g. high or low coefficient of friction). The objective is to somehow push the target object outside the directly reachable radius of the robotic arm. Depending on the situation, the solution to the task can be very simple or quite complex. For example, if the target object is spherical with low friction, the robot could solve the task simply by dropping it against one of the larger blocks, causing it to roll away. However, if the target object is cubic with high friction, it may be necessary for the robot to discover how to construct and use a simple machine such as a ramp — e.g. with the large blocks stacked up and the elongated block placed at one end of the stack as an inclined plane down which the small object can slide.

Bookshelf: In this task, the environment contains a bookshelf with a single book on it. The robot is also provided with two elongated rectangular-prism rods initial placed at random (reachable) locations in the environment. The goal is to knock the book off the bookshelf. However, the book and bookshelf are not only outside the reachable radius of the arm, but they are further than the combined length of the arm and a single rod. However, the robot can solve the task by (e.g.) combining the two rods in an end-to-end configuration using the link macro-action, and then using the combined object to dislodge the book.

Launch-Block: In this task, the environment contains a pre-built rope-and-pulley with one end of the rope connected to an anchor block on the floor and the other attached to a bucket that is suspended in mid-air. A seesaw balances evenly below the bucket, with a target block on the far end of the seesaw. The goal is to launch this target block into the air, above the seesaw surface. The robot could solve this task by (e.g.) gathering all blocks into the bucket and untying the anchor knot so that the bucket will descend onto the near end of the seesaw. However, due to the masses of the blocks and the friction in the seesaw, this can only happen when all five blocks are used.

4.3. Neural Network Settings and Curiosity Metrics

Throughout our experiments, the action selection networks π_θ and V_ϕ are three-layer networks with 64 hidden units each, using the $\tanh$ activation function.

There is a wide range of potential curiosity and novelty metrics, and the optimal metric may be task-dependent. For this reason, we explored a range of such metrics from the recent literature, including: State Estimation (SE) (Mitash et al., 2017), Forward Dynamics (FD) (Burda et al., 2019), and Random Network Distillation (RND) (Choi et al., 2019). The neural network architecture of the curiosity module naturally needed to vary as a function of which metric was chosen. For SE, the curiosity module accepted images of the scene generated from multiple perspectives, in the form of $84 \times 84 \times (3 \cdot n_p)$ pixel arrays (where n_p is the number of perspectives taken), while the architecture was a five-layer convolutional neural network with 3 convolution layers and two fully connected layers. For both FD and RND the architecture consisted of a four-layer MLP with 128 units in each layer. For FD, the inputs were the concatenated vector of system states and actions, while for RND the input simply consisted of the state vector. For fair comparison, the number of trainable parameters in the curiosity modules was approximately equal across curiosity variants.

4.4. Quantitative Results

For each task, we tested CSP in comparison to a variety of baseline approaches. Simple random exploration was tested by assigning a uniform curiosity score to each state and selecting macro-actions from a uniform distribution (CSP-No Curiosity). We also compared CSP to RRT (Lavalle, 1998), a commonly used single-query algorithm used for standard geometric motion planning. We also tested against a vanilla implementation of PPO (Schulman et al., 2017), using the same architecture as the curious action selector shown in Figure 1, but without the tree expansion and sampling module. Finally, we tested a non-planning based but still curiosity-driven DRL model, using the PPO algorithm with the RND curiosity signal (PPO-RND). All metrics and baselines are compared by measuring the number of macro-action samples needed to reach the goal over six different problem instances on five distinct tasks. Implementation details can be found in the supplement.

Overall, we found that CSP was dramatically more effective than the baselines at solving all four task types (Fig. 3). The control algorithms (including the CSP-No Curiosity baseline) were sometimes able to discover solution in the simplest cases (e.g. the 3-Block task). However, they were substantially more variable in terms of the number of samples needed; and they largely failed to achieve solutions in more complex cases within a 10^7-step maximum sample limit. The failure of the random and vanilla PPO/A2C baseliness is not surprising: the tasks we chose here are representative of the kind of long-range planning problems that typically are extremely difficult for standard DRL approaches. The more sophisticated curiosity driven PPO-RND algorithm was able to make headway in a few of the more complex circumstances, but was nonetheless substantially less powerful than the CSP variants.[1]. We ran many additional actor critic and curiosity metric combinations and discussed the results in the supplement. Comparing between curiosity metrics, we found that, while there is some task dependence, Random Network Distillation serves as a good general-purpose curiosity metric achieving the best performance on four of the five tasks (see figure 3). We also performed an ablation on the action selection networks (CSP-RND No AC) to see how beneficial they were to the planning process over random action selection. We found that in all tasks except Bookshelf, CSP performed slightly better with the action selection networks. While not vital for initial planning, they are key for transfer (see sec. 4.6).

4.5. Qualitative Results

We are able to qualitatively compare the exploration patterns of different planning algorithms by examining the graphs generated during the planning process (Fig. 4a). Intriguingly, the topology of the graph structure CSP discovers correspond naturally to qualitatively distinct sub-tasks mak-

[1]RL algorithms are often designed with a multi-episodic environment in mind, in which the external controller repeatedly resets the system to a known state (e.g. in a video game level after the time limit has elapsed). Resetting can often help learning algorithms that would otherwise fail, since it rescues them from unrecoverable states. In our case, such an unrecoverable state arises when objects needed to complete the task are prematurely pushed outside the available radius of the robot arm. The CSP algorithm is easily able to handle this circumstance, because it can expand from previous explored nodes in the state space. To give the baseline algorithms the best chance of working, we thus tested them in two situations: one without trial resetting (the "natural" circumstance for this work), and one with random trial resetting, characterized by a set with probability 1e-4 after each macro-action. Only the PPO-RND algorithm actually benefited from resets, however, and is the only one shown in Fig. 3.

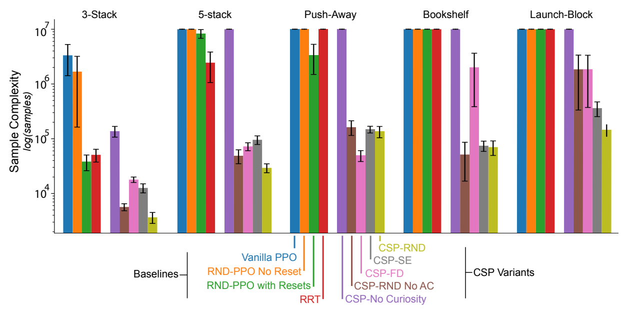

Figure 3. Solution speed for all tested algorithm variants across the five tested tasks. Within each group of 9 bars, the left-most bars represent baselines, while the right-most are the CSP models, including the control No-Curiosity control and several CSP variants with different curiosity metrics (see text for details). The y-axis is on a log scale because the differences between CSP and non-CSP solutions is so great that more subtle differences between various curiosity-metric variants of CSP would otherwise be too small to see. Each bar is computed as the mean of six independent trial runs, and error bars represent the standard error of the mean across trials. We set a maximum number of samples (10^7) in order to ensure termination; in many case the baseline algorithms failed to terminate with a successful solution on any trial.

ing up the overall plan.

In the process of planning, CSP discovers interesting solutions to complex problems, discovering the construction and use of tools and simple machines. Solution paths for each of the tasks are shown in Figure 4b, and video illustrating some representative solutions can be found here: https://youtu.be/7DSW8Dy9ADQ.

Sometimes CSP finds solutions that were unexpected and qualitatively different those imagined by the authors. As an example, we initially developed the PUSH-AWAY task with a spherical ball as a target object, hoping CSP would build a ramp and roll the ball out of the reachability zone. However, CSP instead found a simple solution consisting of dropping the ball directly next to another object in order to get enough horizontal velocity to roll out of the reachability zone. In an attempt to avoid this rather trivial solution, we then switched out the ball for a block with a high coefficient of friction. Now, instead of always building a ramp, CSP sometimes made use of its link macro-action to fix the block to one end of the plank and orient it so that the block was held outside the reachability zone. Once the link macro-action was disabled, ramp-building behavior robustly emerged.

4.6. Task Transfer

A central aspect of human intelligence is the ability to improve at solving problems over time and to use knowledge gained from solving one problem to more efficiently solve related problems. For this reason, we were curious

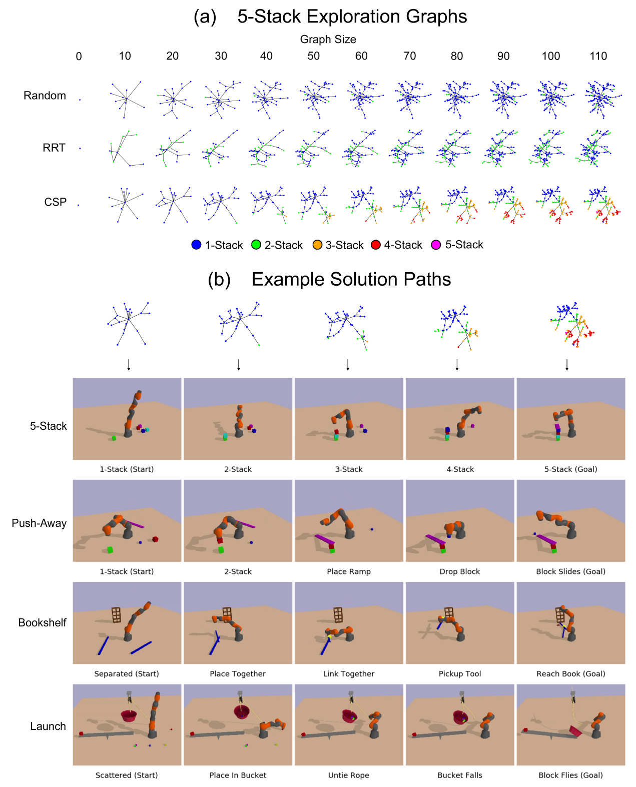

Figure 4. **a.** Search graphs for the 5-Stack task for CSP, Random (CSP-No Curiosity), and RRT planning algorithms. These example search graphs demonstrate how CSP utilizes the novelty score to oversample unseen and interesting configurations such as stacked blocks, leading to faster solution convergence. **b.** Example solution trajectories found by CSP for three of the tasks with annotations to explain each of the steps in the trajectory.

whether CSP could transfer knowledge between problem instances with different initial conditions, and between different but related problems. We evaluated transfer both the within-task and between-task using 3-STACK, 5-STACK, and PUSH-AWAY tasks. We selected these tasks because they all share a common essential skill: stacking blocks.

We tested transfer from each learnable component of the system individually, to identify which components of the system can be effectively reused between problems, including (i) the baseline "no transfer" condition, where neither the curiosity module nor the action selection networks are transferred from another problem instance; (ii) condition where just the curiosity module or action selection networks were transferred; and (iii) a full transfer condition where both the action selection networks and the curiosity module are transferred between tasks.

Results (Fig. 5) show that transferring the curiosity module alone slightly improves planning ability between instances of the same task, but has a minimal effect and can even

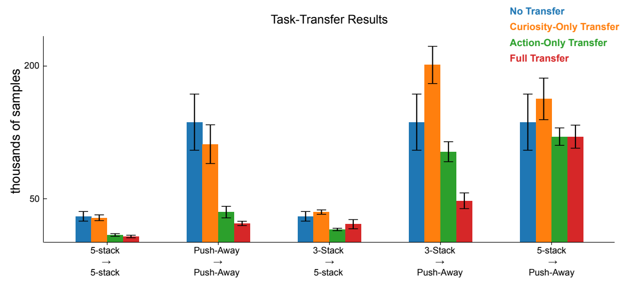

Figure 5. Inter-task and between-task transfer efficiency measured by the number of samples needed to reach the goal, for each of several transfer policies (only curiosity module, only action selection module, and full network transfer). The CSP-RND variant is used for all cases. Within each group of bars for a given task, the difference between blue bar (No Transfer) and other bars represents transfer gain (note that the y-axis is on a logarithmic scale). Each condition was run 6 times and error bars represent standard error of the mean over runs.

be detrimental in the case of between-task transfer. On the other hand, transferring the action selection networks leads to a large increase in efficiency in all tasks except for 3-STACK. (The 3-STACK task is likely unaffected by transfer because it is solved so quickly that the networks have little time to train.) Full transfer results in transfer performance improvements similar to that of transferring the action selection network alone. Gains arose for qualitatively identifiable reasons e.g. once CSP learned to solve the stacking problem, it tries stacking macro-actions much more frequently as an initial guess, which is naturally useful for solving the Push-Away task. Transfer gains are reflected by the fact that the tree search procedure has learned to very effectively reduce the task tree, a particularly dramatic example of which is illustrated in Fig. 5b.

5. Conclusion

In this work, we introduce the CSP algorithm, a fusion of classical task-planning and deep RL approaches that is capable of flexible long-range multi-step planning in sparse reward settings. CSP consists of two learnable components which aim to maximize curiosity in action selection and state exploration. The first component is the action selector networks which reduces sampling of infeasible or uninteresting effects in favor of macro-actions and parameters which lead to interesting and unseen effects. The second component is a curiosity module which guides exploration of the state tree toward novel state configurations by increasing the probability that those nodes will be expanded. We show that the addition of these components not only speeds up planning when compared to random action selection and reinforcement learning baselines but also has the ability to make otherwise intractable problems solvable. We also systematically examine the effect of different forms of curiosity on task performance, finding RND is the most effective overall. Finally, we look at the transferability of solutions to new instances of the same general problem and to related but different problems, showing that networks trained to select actions states which result in interesting configurations perform better than those which are randomly initialized.

Despite its initial successes, CSP has a number of key limitations that will need to be addressed in future work. As a pure planning algorithm, CSP does not attempt to solve a directed learning problem over the course of many trials; when very large numbers of trials are available for training, it is plausible that Deep RL approaches would begin to catch up with and eventually exceed CSP performance. A very natural next step will be to combine CSP with a cross-trial learning algorithm to obtain the best of both worlds. It will also be key to show that CSP is able to function effectively when only a non-deterministic and noisy future prediction module is available, rather than the unrealistic perfect black-box predictor used in this work. It will be especially important to determine if CSP is compatible with a learned future predictor, and of interest to determine if CSP-generated plans could help accelerate the learning of such a predictor simultaneously while CSP modules are themselves learned. Another key direction for future work will be to apply a CSP-like procedure to the discovery of macro-actions themselves (Barto et al., 2004; Machado et al., 2017), resulting in a hierarchical multi-timescale procedure in which more and more complex plans become routinized as macro-actions. Finally, it will be of interest to compare the behavior sequences generated by CSP to data from experiments measuring patterns of play and discovery in both human children and adults (Gopnik et al., 2009; Begus et al., 2014), as both the similarities and differences between human decision making and exploration and algorithmic outputs will help inform the development of improved flexible and efficient planning algorithms.

References

Achiam, J. and Sastry, S. S. Surprise-based intrinsic motivation for deep reinforcement learning. *ArXiv*, abs/1703.01732, 2017.

Arulkumaran, K., Deisenroth, M. P., Brundage, M., and Bharath, A. A. Deep reinforcement learning: A brief survey. *IEEE Signal Processing Magazine*, 34:26–38, 2017.

Barto, A. G., Singh, S., and Chentanez, N. Intrinsically motivated learning of hierarchical collections of skills. In *Proceedings of International Conference on Developmental Learning (ICDL)*. MIT Press, Cambridge, MA, 2004.

Begus, K., Gliga, T., and Southgate, V. Infants learn what they want to learn: Responding to infant pointing leads to superior learning. *PLOS ONE*, 9(10):1–4, 10 2014. doi: 10.1371/journal.pone.0108817.

Bellemare, M., Srinivasan, S., Ostrovski, G., Schaul, T., Saxton, D., and Munos, R. Unifying count-based exploration and intrinsic motivation. In *Advances in Neural Information Processing Systems*, pp. 1471–1479, 2016.

Bellman, R. A Markovian decision process. *Journal of Mathematics and Mechanics*, 6:679–684, 1957.

Burda, Y., Edwards, H., Pathak, D., Storkey, A., Darrell, T., and Efros, A. A. Large-scale study of curiosity-driven learning. In *ICLR*, 2019.

Chitnis, R., Hadfield-Menell, D., Gupta, A., Srivastava, S., Groshev, E., Lin, C., and Abbeel, P. Guided search for task and motion plans using learned heuristics. In *2016 IEEE International Conference on Robotics and Automation, ICRA 2016*, volume 2016-June, pp. 447–454. Institute of Electrical and Electronics Engineers Inc., 6 2016. doi: 10.1109/ICRA.2016.7487165.

Choi, J., Guo, Y., Moczulski, M., Oh, J., Wu, N., Norouzi, M., and Lee, H. Contingency-aware exploration in reinforcement learning. In *International Conference on Learning Representations*, 2019. URL https://openreview.net/forum?id=HyxGB2AcY7.

Coumans, E. Bullet physics simulation. In *ACM SIGGRAPH 2015 Courses*, SIGGRAPH '15, New York, NY, USA, 2015. ACM. ISBN 978-1-4503-3634-5. doi: 10.1145/2776880.2792704. URL http://doi.acm.org/10.1145/2776880.2792704.

Dantam, N. T., Kingston, Z. K., Chaudhuri, S., and Kavraki, L. E. Incremental task and motion planning: A constraint-based approach. In *Robotics: Science and Systems*, 2016.

Deisenroth, M., Rasmussen, C., and Fox, D. Learning to control a low-cost manipulator using data-efficient reinforcement learning. 06 2011. doi: 10.15607/RSS.2011.VII.008.

Fikes, R. E. and Nilsson, N. J. Strips: A new approach to the application of theorem proving to problem solving. *Artificial Intelligence*, 2:189, 1971.

Garrett, C. Pybullet planning. 2018.

Garrett, C. R., Lozano-Pérez, T., and Kaelbling, L. P. Sampling-based methods for factored task and motion planning. *CoRR*, abs/1801.00680, 2018. URL http://arxiv.org/abs/1801.00680.

Gopnik, A., Meltzoff, A., and Kuhl, P. *The Scientist In The Crib: Minds, Brains, And How Children Learn*. HarperCollins, 2009. ISBN 9780061846915.

Gravot, F., Cambon, S., and Alami, R. asymov: A planner that deals with intricate symbolic and geometric problems. In Dario, P. and Chatila, R. (eds.), *Robotics Research. The Eleventh International Symposium*, pp. 100–110, Berlin, Heidelberg, 2005. Springer Berlin Heidelberg. ISBN 978-3-540-31508-7.

Haber, N., Mrowca, D., Fei-Fei, L., and Yamins, D. L. Learning to play with intrinsically-motivated self-aware agents. In *Advances in Neural Information Processing Systems*, 2018.

Helmert, M. The fast downward planning system. *Journal of Artificial Intelligence Research*, 26:191–246, 2006.

Hertle, A., Dornhege, C., Keller, T., and Nebel, B. Planning with semantic attachments: An object-oriented view. In *Proceedings of the 20th European Conference on Artificial Intelligence*, ECAI'12, pp. 402–407, Amsterdam, The Netherlands, The Netherlands, 2012. IOS Press. ISBN 978-1-61499-097-0. doi: 10.3233/978-1-61499-098-7-402. URL https://doi.org/10.3233/978-1-61499-098-7-402.

Hessel, M., Modayil, J., van Hasselt, H., Schaul, T., Ostrovski, G., Dabney, W., Horgan, D., Piot, B., Azar, M. G., and Silver, D. Rainbow: Combining improvements in deep reinforcement learning. In *AAAI*, 2017.

Hoffmann, J. and Nebel, B. The ff planning system: Fast plan generation through heuristic search. *J. Artif. Int. Res.*, 14(1):253–302, May 2001. ISSN 1076-9757. URL http://dl.acm.org/citation.cfm?id=1622394.1622404.

Kaelbling, L. P. and Lozano-Pérez, T. Integrated task and motion planning in belief space. *Int. J. Rob. Res.*, 32 (9-10):1194–1227, August 2013. ISSN 0278-3649. doi: 10.1177/0278364913484072. URL http://dx.doi.org/10.1177/0278364913484072.

Kakade, S. M. *On the sample complexity of reinforcement learning*. PhD thesis, University of London London, England, 2003.

Kavraki, L., Svestka, P., Latombe, J., and Overmars, M. Probabilistic roadmaps for path planning in high-dimensional configuration spaces. *Robotics and Automation, IEEE Transactions on*, 12:566 – 580, 09 1996. doi: 10.1109/70.508439.

Kim, B., Kaelbling, L., and Lozano-Perez, T. Guiding search in continuous state-action spaces by learning an action sampler from off-target search experience. In *Proceedings of the 32th AAAI Conference on Artificial Intelligence (AAAI). To appear*. AAAI Press, 2018. URL http://lis.csail.mit.edu/pubs/kim-aaai18.pdf.

Kim, B., Kaelbling, L. P., and Lozano-Perez, T. Adversarial actor-critic method for task and motion planning problems using planning experience. In *AAAI Conference on Artificial Intelligence (AAAI)*, 2019. URL http://lis.csail.mit.edu/pubs/kim-aaai19.pdf.

Kingston, Z., Moll, M., and Kavraki, L. E. Sampling-based methods for motion planning with constraints. *Annual Review of Control, Robotics, and Autonomous Systems*, 1(1):159–185, 2018. doi: 10.1146/annurev-control-060117-105226. URL https://doi.org/10.1146/annurev-control-060117-105226.

Kroemer, O. and Sukhatme, G. S. Learning spatial preconditions of manipulation skills using random forests. *2016 IEEE-RAS 16th International Conference on Humanoid Robots (Humanoids)*, pp. 676–683, 2016.

Kuffner, J. and LaValle, S. Rrt-connect: An efficient approach to single-query path planning. volume 2, pp. 995–1001, 01 2000. doi: 10.1109/ROBOT.2000.844730.

Kulkarni, T. D., Narasimhan, K., Saeedi, A., and Tenenbaum, J. Hierarchical deep reinforcement learning: Integrating temporal abstraction and intrinsic motivation. In *Advances in neural information processing systems*, pp. 3675–3683, 2016.

Lavalle, S. M. Rapidly-exploring random trees: A new tool for path planning. 1998.

Li, R., Jabri, A., Darrell, T., and Agrawal, P. Towards practical multi-object manipulation using relational reinforcement learning. In *arXiv preprint arXiv:1912.11032*, 2019.

Lillicrap, T. P., Hunt, J. J., Pritzel, A., Heess, N. M. O., Erez, T., Tassa, Y., Silver, D., and Wierstra, D. Continuous control with deep reinforcement learning. *CoRR*, abs/1509.02971, 2015.

Luh, J. Y. S., Walker, M. W., and Paul, R. P. C. On-Line Computational Scheme for Mechanical Manipulators. *Journal of Dynamic Systems, Measurement, and Control*, 102(2):69–76, 06 1980. ISSN 0022-0434. doi: 10.1115/1.3149599. URL https://doi.org/10.1115/1.3149599.

Machado, M. C., Bellemare, M. G., and Bowling, M. A laplacian framework for option discovery in reinforcement learning. In *Proceedings of the 34th International Conference on Machine Learning-Volume 70*, pp. 2295–2304. JMLR. org, 2017.

Mitash, C., Bekris, K. E., and Boularias, A. A self-supervised learning system for object detection using physics simulation and multi-view pose estimation. In *IEEE/RSJ International Conference on Intelligent Robots and Systems (IROS)*, Vancouver, Canada, 09/2017 2017. URL https://www.cs.rutgers.edu/~kb572/pubs/physics_object_detection.pdf.

Mnih, V., Kavukcuoglu, K., Silver, D., Rusu, A. A., Veness, J., Bellemare, M. G., Graves, A., Riedmiller, M., Fidjeland, A. K., Ostrovski, G., et al. Human-level control through deep reinforcement learning. *Nature*, 518(7540): 529, 2015.

Mnih, V., Badia, A. P., Mirza, M., Graves, A., Lillicrap, T. P., Harley, T., Silver, D., and Kavukcuoglu, K. Asynchronous methods for deep reinforcement learning. *CoRR*, abs/1602.01783, 2016. URL http://arxiv.org/abs/1602.01783.

Mrowca, D., Zhuang, C., Wang, E., Haber, N., Fei-Fei, L., Tenenbaum, J. B., and Yamins, D. L. K. Flexible neural representation for physics prediction. In *NeurIPS*, 2018.

Nair, A., McGrew, B., Andrychowicz, M., Zaremba, W., and Abbeel, P. Overcoming exploration in reinforcement learning with demonstrations. pp. 6292–6299, 05 2018. doi: 10.1109/ICRA.2018.8463162.

Osband, I., Blundell, C., Pritzel, A., and Van Roy, B. Deep exploration via bootstrapped dqn. In *Advances in neural information processing systems*, pp. 4026–4034, 2016.

Pathak, D., Agrawal, P., Efros, A. A., and Darrell, T. Curiosity-driven exploration by self-supervised prediction. In *Proceedings of the IEEE Conference on Computer Vision and Pattern Recognition Workshops*, pp. 16–17, 2017.

Puterman, M. L. *Markov Decision Processes—Discrete Stochastic Dynamic Programming*. John Wiley & Sons, Inc., New York, NY, 1994.

Riedmiller, M. A., Hafner, R., Lampe, T., Neunert, M., Degrave, J., de Wiele, T. V., Mnih, V., Heess, N., and Springenberg, J. T. Learning by playing - solving sparse reward tasks from scratch. *CoRR*, abs/1802.10567, 2018. URL http://arxiv.org/abs/1802.10567.

Schmidhuber, J. Formal theory of creativity, fun, and intrinsic motivation (19902010). *IEEE Transactions on Autonomous Mental Development*, 2:230–247, 2010.

Schulman, J., Wolski, F., Dhariwal, P., Radford, A., and Klimov, O. Proximal policy optimization algorithms. *CoRR*, abs/1707.06347, 2017. URL http://arxiv.org/abs/1707.06347.

Silver, D., Huang, A., Maddison, C. J., Guez, A., Sifre, L., van den Driessche, G., Schrittwieser, J., Antonoglou, I., Panneershelvam, V., Lanctot, M., Dieleman, S., Grewe, D., Nham, J., Kalchbrenner, N., Sutskever, I., Lillicrap, T. P., Leach, M., Kavukcuoglu, K., Graepel, T., and Hassabis, D. Mastering the game of go with deep neural networks and tree search. *Nature*, 529:484–489, 2016.

Singh, S. P., Barto, A. G., and Chentanez, N. Intrinsically motivated reinforcement learning. In *Advances in neural information processing systems*, pp. 1281–1288, 2005.

Srivastava, S., Fang, E., Riano, L., Chitnis, R., Russell, S., and Abbeel, P. Combined task and motion planning through an extensible planner-independent interface layer. *Proceedings - IEEE International Conference on Robotics and Automation*, pp. 639–646, 1 2014. ISSN 1050-4729. doi: 10.1109/ICRA.2014.6906922.

Thrun, S. B. Efficient exploration in reinforcement learning. 1992.

Toussaint, M., Allen, K. R., Smith, K. A., and Tenenbaum, J. B. Differentiable physics and stable modes for tool-use and manipulation planning – extended abstract, 2019. Sister Conference Best Paper Track – Extended abstract of the R:SS'18 paper.

Vega-Brown, W. and Roy, N. Asymptotically optimal planning under piecewise-analytic constraints. 2018.

Vinyals, O., Babuschkin, I., Czarnecki, W. M., Mathieu, M., Dudzik, A. J., Chung, J., Choi, D. H., Powell, R. W., Ewalds, T., Georgiev, P., Oh, J., Horgan, D., Kroiss, M., Danihelka, I., Huang, A., Sifre, L., Cai, T., Agapiou, J. P., Jaderberg, M., Vezhnevets, A. S., Leblond, R., Pohlen, T., Dalibard, V., Budden, D., Sulsky, Y., Molloy, J., Paine, T. L., Gulcehre, C., Wang, Z., Pfaff, T., Wu, Y., Ring, R., Yogatama, D., Wünsch, D., McKinney, K., Smith, O., Schaul, T., Lillicrap, T. P., Kavukcuoglu, K., Hassabis, D., Apps, C., and Silver, D. Grandmaster level in starcraft ii using multi-agent reinforcement learning. *Nature*, pp. 1–5, 2019.

Wang, Z., Garrett, C. R., Kaelbling, L. P., and Lozano-Perez, T. Active model learning and diverse action sampling for task and motion planning. In *International Conference on Intelligent Robots and Systems (IROS)*, 2018. URL http://lis.csail.mit.edu/pubs/wang-iros18.pdf.

A. Curiosity Metrics

A.1. State Estimation Curiosity

The objective of the state estimation curiosity module is to estimate the underlying state of the world through a set of visual observations. State configurations that are visually distinct from previously seen configurations will lead to high losses. The curiosity module and loss function are defined as follows.

$$H_\beta : Im \mapsto \mathcal{S}$$

$$\mathcal{L}_i = \|H_\beta(Im_i) - s_i\|_2^2$$

Where Im is the space of $84 \times 84 \times 3 \cdot n_p$ matrices containing n_p images captured from various perspectives in the scene, $s \in S$ denotes the state, and i is an index into the batch. In our experiments, we used a single top-down perspective ($n_p = 1$).

A.2. Forward Dynamics Curiosity

The objective of the forward dynamics curiosity module is to estimate future states given current states and actions. Given deterministic physics, actions modify states deterministically. Therefore, it is theoretically possible to estimate a future state from an action and the current state. Rare or unpredictable object-object interaction will yield the highest loss in dynamics prediction and therefore will be sought out by the curiosity module. The curiosity module and loss function are described as follows.

$$H_\beta : S \mapsto \mathcal{S}$$

$$f : \mathcal{S} \times \mathcal{A} \mapsto \mathcal{S}$$

$$\mathcal{L}_i = \|H_\beta(s_i) - f(s_i, a_i)\|_2^2$$

Where f is the deterministic dynamics model which maps a state and action at t to a state at time $t + \tau$ for some fixed τ.

A.3. Random Network Distillation Curiosity

Random Network Distillation (RND) is a recently proposed method for obtaining state-space coverage. This is achieved by training a model to fit some fixed random transformation of the input data. The RND curiosity module achieves low loss when it matches the transformation. This results in high curiosity module loss for unseen states.

$$H_\beta, \Phi_\beta : S \mapsto \mathcal{S}$$

$$\mathcal{L}_i = \|H_\beta(s_i) - \Phi(s_i)\|_2^2$$

Where Φ is the fixed mapping that is initialized with random parameters. Among other mappings including random linear and non-linear mappings with uniformly and gaussian distributed weights, we found that the best performing mapping was a random permutation of the state vector.

B. Network Structures and Hyperparameters

B.1. Actor Critic Policy and Value Networks

The structure of the policy network is a multilayer perceptron model with three layers. The input size is the dimensionality of the state space and the output size is equivalent to the dimensionality of the action space. Action space and state space dimensionality are described in more detail below. The hidden layers each have 64 hidden units with $tanh$ activation functions. The the value network has an equivalent architecture but with an output size of one.

For PPO and A2C training, we used the same hyperparameters during action selection network training and baseline experimentation. For PPO we used a batch size of 128 with 1024 samples collected per update, $\gamma = 0.9$, $lr = 7e - 4$, $\varepsilon = 0.2$. We also selected value and entropy coefficients of 0.5 and 0.0 respectively and restricted the magnitude of the gradient to 0.5. For each batch, we did 4 PPO epoch updates. For A2C, we used the same learning rate and coefficients as PPO.

B.2. State Estimation Convolution Network

The state estimation network takes in visual input from perspectives in the scene and outputs an estimated state. We achieved this image to state mapping using a convolutional neural network with three convolutional layers and two fully connected layers, all with $ReLU$ nonlinearities. Because we used a single perspective for all of our experiments, the input size is $84 \times 84 \times 3$ and the output size is the dimensionality of the state space. The convolutional layers have kernel sizes of 8, 4, 3 and strides of 4, 2, 1. The fully connected layers each have 128 hidden units.

B.3. Forward Dynamics Network

The forward dynamics network maps s_t, a_t to $s_{t+\tau}$. This is achieved using a multilayer perceptron model with 3 layers, 64 hidden units per layer and $tanh$ activation functions. The input size is the sum of the action and state dimensionality and the output size is the dimensionality of the state.

B.4. RND Network

The RND network maps states to transformed states. The size we used for the transformed state is equivalent to the size of the state. Therefore, the input and output sizes are both equivalent to the dimensionality of the state. The architecture consisted of a three layer multilayer perceptron model with $tanh$ activation functions and 64 hidden units for each hidden layer.

B.5. Universal Curiosity Module Hyperparameters

For training the curiosity networks, we used an Adam optimizer with a learning rate of 5×10^{-5}, a batch size of 128, and 1024 samples per update. We also found that performance was higher when we used an adaptive number of samples per update. The number of samples is increased until the loss is below a threshold after training. This improves CSP by giving the curiosity network time to train to baseline before adding nodes to the tree.

C. Task Specific State Space and Action Space

C.1. Stack State

This set of tasks consists of k cubes. Each cube has it's own $SE(3)$ configuration parameterized by three positional degrees of freedom and three euclidean rotational degrees of freedom. When the linking macro-action is enabled, the state also contains indicator values for each pairwise object combination.

C.2. Push-Away State

This task contains two larger cubes, one smaller cube, and one elongated, flat rectangular prism. Again, the dimensionality of the state space is $SE(3)$ for each object along with pairwise indicators when the linking macro-action is enabled.

C.3. Bookshelf State

This task contains two rods elongated rectangular prism rods and a rectangular prism book, each with a $SE(3)$ configuration space and pairwise linking. Linking is always enabled for this task because it is required to complete it.

C.4. Launch-Block State

The state space for this task contains five small cubes, one larger cube that sits at the end of the seesaw, and the angle of the seesaw itself. Each of the cubes has an $SE(3)$ configuration space and the seesaw has a bounded real configuration with a single degree of freedom.

C.5. Transfer States

When comparing between tasks, the action spaces and state spaces need matching dimensionality to ensure the networks could be substituted. We achieved this by making sure each problem instance had an equivalent number of objects, even if it was unnecessary to use all objects to complete the task. For the transfer results stated in this paper, this equated to using five objects for each task.

C.6. Action Spaces

When both linking and pick-place macro-actions are enabled, the action space needs to contain information for choosing which object to move (k total), the goal pose of the object (dof), which of the $\binom{k}{2}$ object pairs to link or unlink , and which macro-action to select (linking or pick-place). Therefore, the dimensionality of the action space is $\binom{k}{2} + (dof + 1) \cdot k + 2$. The macro-action, link, and object discrete variables are chosen by performing an argmax over the respective section of the action space. If a link macroaction is selected between two objects that are already linked, this is considered an unlink action and the constraint between the two objects is removed. If a link is chosen between two objects which aren't in contact, then the action is considered to be infeasible. For implementation simplicity, we use k^2 variables for the linking indicator rather than $\binom{k}{2}$ and ignore any redundant pairs.

D. Baselines

In addition to the CSP variants, we compared the performance of CSP to a number of deep reinforcement learning and motion planning baselines. The implementation of these baselines is explained in detail below.

D.1. RRT

The overall objective of RRT is to explore the configuration space by sampling a feasible configuration from some distribution over the configuration space, selecting the node that is closest to that configuration in the search tree, executing an action primitive from that node, and adding the resulting node to the search tree (Lavalle, 1998). Because the problem setup is such that the effects of individual macro-actions are unknown, direct analytic control is impossible. Thus, the action is selected randomly from a uniform distribution over the space of parameterized macro-actions.

D.2. Vanilla DRL

We used vanilla implementations of PPO (Schulman et al., 2017) and A2C (Mnih et al., 2016) using the same hyperparameters described in Section B.1. A major shortcoming when using these algorithms for planning is that they are unable to revert to previously explored states and thus will often get stuck with one or multiple of the objects in the scene becoming unreachable. Therefore, we implemented a probabilistic resetting policy such that the environment resets to the initial problem state with probability 1e-4. While training, the environment was also reset to the starting state when a goal state was reached. The agent received a reward of 1 after reaching the goal state and a reward of 0 otherwise. The quantitative results reported were the number of steps taken by the trained policy in six unseen initial configurations after $5e5$ steps of training. The primary reason for the failure of vanilla DRL baselines was that the reward is far too sparse in each of the problems to generalize to unseen configurations. In many of the problems, the DRL algorithms failed to find even a single positive example for which it received reward.

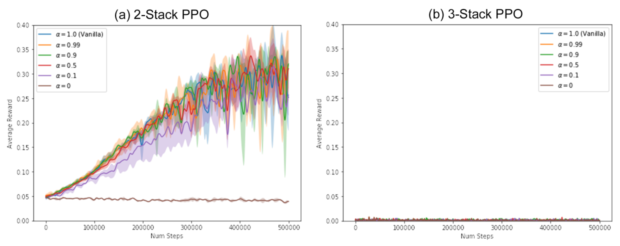

Figure 6. Reward curves during PPO training for (a) 2-Stack and (b) 3-Stack tasks using different intrinsic/extrinsic reward weighting α. These results demonstrate that our actor-critic DRL implementation is correct and functioning in environments where the reward it not sparse, but fails to learn in sparse-reward environments even when the reward includes intrinsic curiosity.

In order to validate that our actor-critic implementation was functioning correctly, we tested it on the simpler 2-Stack problem in which the reward was not too sparse for policy learning. The 2-stack problem was solved by our actor critic implementation but the sparse-reward 3-stack problem could not be solved (see Fig 6).

D.3. Curious DRL

One potential method for overcoming the sparse reward problem in DRL is to "densify" the reward space by adding an intrinsic reward that incentivizes environmental exploration (Choi et al., 2019). In order to test this, we modified the vanilla PPO implementation to use the sum of extrinsic reward (R_e) and RND world model loss trained alongside the actor-critic networks (R_i) as the total reward ($R_t = \alpha R_e + (1 - \alpha) R_i$) for the DRL agent. We experiment with several values of the alpha hyperparameter ($\alpha = 0.0, 0.1, 0.5, 0.9, 0.99, 1.0$), with vanilla PPO being a special case where $\alpha = 1$, and found no clear benefit over vanilla training in the quantitative results (see Fig 6).

D.4. Code

All of the code for this project can be found here:
https://github.com/neuroailab/CuriousSamplePlanner